Exp Brain Res (1987) 68: 249–259

Experimental Brain Research

Diversity of complex cell responses to even- and odd-symmetric luminance profiles in the visual cortex of the cat

J.P. Gaska[1], D.A. Pollen[1], and P. Cavanagh[2]

[1] Neurobiology Laboratory, Department of Neurology, University of Massachusetts Medical School, Worcester, MA 01605, USA
[2] Département de Psychologie, Université de Montréal, Montréal, Québec, Canada

Summary. We have tested the hypothesis that complex cell receptive fields are made up of subfields which, for a given cell, have either exclusively even or exclusively odd symmetry. To do this we have measured the response of complex cells in the visual cortex of the cat to members of pairs of spatially limited even-symmetric stimuli (single light and dark bars) and pairs of odd-symmetric stimuli ("light-dark" and "dark-light" double bars) successively drifting across their receptive fields. The strength of a cell's response was estimated by measuring the sum of all spikes produced by a stimulus. Some complex cells respond about equally to single light and dark bars; others respond appreciably more to either the light or dark bar. The central tendency of average response histograms was estimated by measuring the mean with respect to position across the width of the receptive field. Many complex cells show distinct spatial offsets between the mean for narrow single light and that for dark bars as well as between means to double bars of opposite phase. Combined offset plots were constructed with the spatial offsets between means for single light bars and single dark bars along the x axis and the offsets between means to double bars of opposite phase along the y axis. There is significant scatter in the combined offset points; some falling at the origin, some at significant distances from the origin along the axes, and others well within each of the four quadrants. These diverse localizations in the offset plots rule out the simple models of complex cell spatial substructure described above and, therefore, imply considerable heterogeneity within the population of complex cells.

Key words: Vision – Visual cortex – Spatial tuning – Complex cell – Complex cell substructure

Offprint requests to: D.A. Pollen (address see above)

Introduction

Spatial information processing across the width dimension of simple cells can, except for cross-spatial frequency interactions (DeValois and Tootell 1983) and a threshold, be reasonably well accounted for by a stage of linear summation of the input weighted by the response sensitivity profile followed by truncation of the output (Movshon et al. 1978a; Andrews and Pollen 1979; Maffei et al. 1979). Conversely, the overall response of a complex cell to visual stimuli can be characterized by certain non-linearities introduced by truncation at an earlier stage; nevertheless, the contributing subunits may individually process spatial information linearly before their responses are truncated (Movshon et al. 1978b). It is not yet known whether a single complex cell receives input from subunits all having the same response sensitivity profiles (e.g. all even- or odd-symmetric) (Cavanagh 1984) or from several types of subunits (Pollen et al. 1985), nor whether there exists a functional heterogeneity within the class of complex cells. An increased understanding of the substructure of the complex cell would be of interest not only for its own sake but because it might impose restraints upon proposals for the function of complex cells. One specific hypothesis that we will test and subsequently reject is that the receptive fields of complex cells are made up exclusively of subfields all having either even- or odd-symmetry.

Our approach begins with an analysis of the contributing subunits to complex cells. We accept the conclusion of Movshon et al. (1978b) that the subunits contributing to complex cells are linear spatial filters whose responses are subsequently rectified. In addition, we make the tentative simplifying assumption that the outputs from subunits are summed to produce the complex cell response as in the model of Spitzer and Hochstein (1985a), however, we are aware that the issue of whether subunit interactions

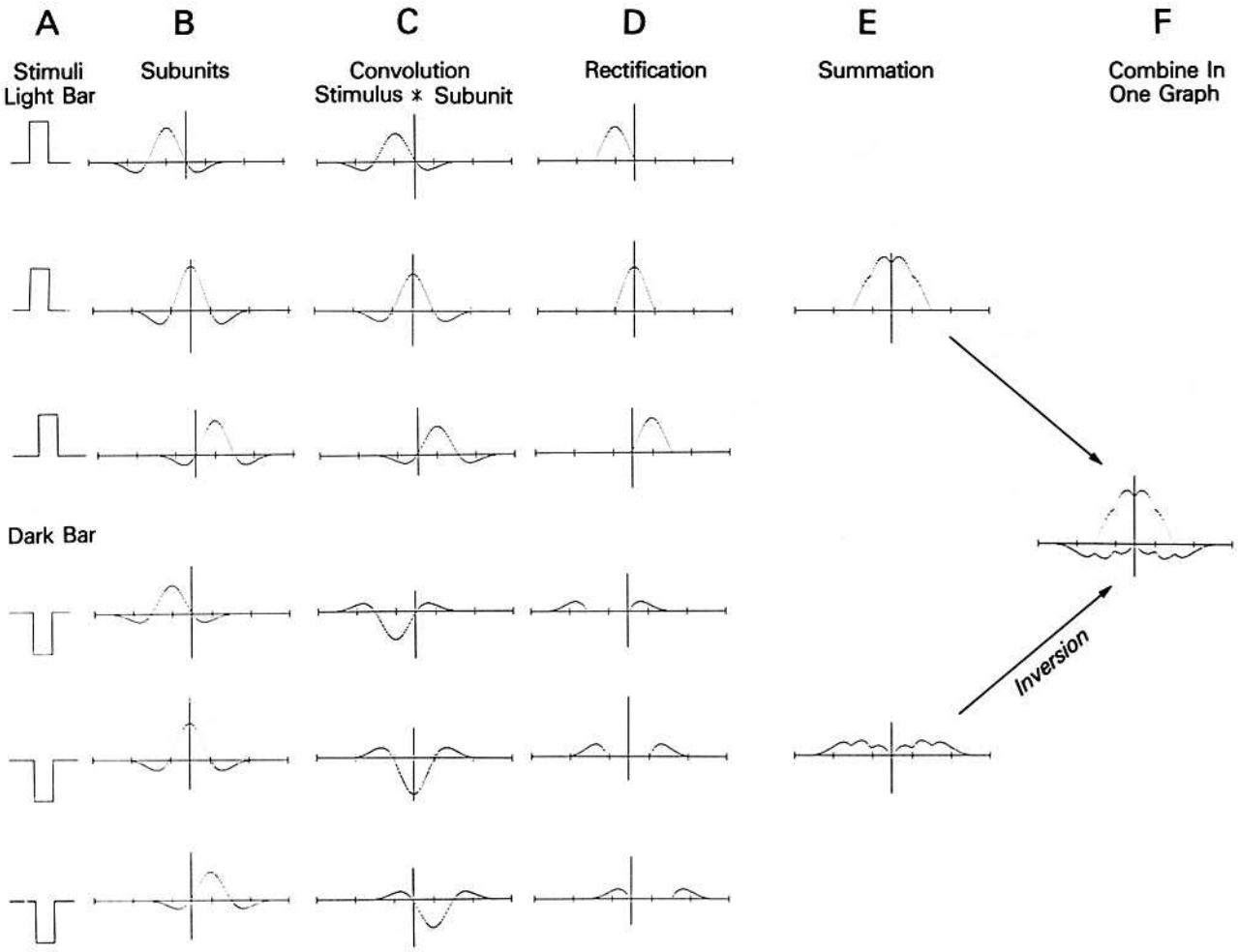

Fig. 1A–F. Illustration of the sequence of convolution of light and dark bar stimuli (**A**) with three adjacent subunits (**B**) to produce responses (**C**) followed by rectification of each response (**D**) and subsequent summation of adjacent rectified responses to light bar (**E**, upper) and to dark bar (**E**, lower). The summed rectified response to the dark bar is then inverted and combined with the non-inverted response to the light bar (**F**). The upper three rows show responses to the light bar for three adjacent subunits, the lower three traces similarly so for the dark bar. The subunits were calculated from a Gabor function with spatial frequency full bandwidths of 2 octaves at half amplitude.

involve nonlinearities has not been resolved. We assume that the peaks and bandwidths of the spatial frequency tuning curves of the contributing subunits are close to those for the overall complex cell and that the contributions of each subunit across the receptive field are weighted by some function (possibly Gaussian) whose exact form need not be examined here.

We then successively drift members of pairs of spatially-limited even-symmetric stimuli (single light and dark bars) and pairs of odd-symmetric stimuli ("light-dark" and "dark-light" double bars) across the receptive fields of complex cells. In the space domain the single bar stimuli probe the positions and properties of the complex cell subunits themselves; the double bar stimuli reveal properties of the derivatives of the line-weighting functions of the contributing subgroups. In the spatial frequency domain, all component spatial frequencies of the single light and dark bars are in plus or minus cosine phase respectively at the center of the stimulus, whereas all component frequencies of the two double bars are in either plus or minus sine phase at the stimulus center. The stimuli are therefore able to probe the sensitivity of the complex cell to the relative phase offsets among the component spatial frequencies of the stimuli. Taken together, these four stimuli permit a novel and robust approach for analyzing the contributions of subunits to complex cells.

Methods

Ten adult cats were anesthetized with ketamine 20 mg/kg for the insertion of an intravenous cannula. A short-acting barbiturate, Brevital 3 mg/kg, was given in general anesthetic doses as needed for a tracheotomy. Surgical levels of general anesthesia were then maintained by intravenous injection of sodium pentobarbitone. A local anesthetic was applied at pressure points before the animal was placed in a stereotactic apparatus and a long-acting local anesthetic was injected into the scalp prior to incision. The EEG and ECG were monitored. A small trephine hole was made through the cranium so that electrode penetrations could be made between coordinates P 3.0–P 5.0 and L 1.0–1.5. A small durotomy was made, and a tungsten in parylene microelectrode was lowered under visual guidance with the aid of a binocular operating microscope until the electrode tip rested just above the pulsating cortex. The small chamber around the trephine hole was then sealed. The microelectrode was later advanced, using a high acceleration stepping motor in 10 μ advance steps, until the first sign of cortical activity was found. The microelectrode was then withdrawn until signs of unit activity were no longer present. This location was assigned a depth of zero. Upon the completion of surgery, the animal was paralyzed with pancuronium bromide (0.2mg/kg/h) and respired on a mixture of 70% nitrous oxide and 30% oxygen with supplemental pentobarbital, in increments of 1 mg/kg, as needed to eliminate pain or discomfort as judged by precluding an arousal pattern in the EEG or an abnormal increase in the heart rate.

Our general techniques for recording and optics have been described in a recent publication (Foster et al. 1985). All cells included here were recorded at retinal eccentricities within 5° of the area centralis.

Visual stimulation

Stimuli were presented on the face of a Tektronix 608 display monitor with a P4 phosphor. The X, Y, and Z inputs to the oscilloscope were taken from a cathode-ray tube image generator (Innisfree, Inc.) under computer control which was used to produce a one dimensional drifting sinusoidal grating or the single and double bars of arbitrary orientation and velocity. The mean luminance of the oscilloscope face was 50 cd/m^2. Grating contrast was defined using the Michaelson formula $C_{grating} = (L_{max}-L_{min})/(L_{max} + L_{min})$. Within any given spatial frequency selectivity study, contrast was maintained constant and generally ranged from 20–30%. Bar contrast was defined as the luminance increase (light bar) or luminance decrease (dark bar) of the bar above or below 50 cd/m^2 divided by 50 cd/m^2. Our standard bar contrasts were ±35%, well within the linear range of the display monitor at the mean luminance used.

Stimulus terminology

Two of the four stimuli we used were single bars having, therefore, even symmetry. We will also refer to these stimuli as cosine phase stimuli because all of the component spatial frequencies are in cosine phase at the center of the stimulus. The light, or positive bar is in +cosine phase and the dark or negative bar is in –cosine phase. The remaining two stimuli were double bars having odd symmetry. These are sine phase stimuli as all the spatial frequency components are in sine phase at the center. The dark/light or positive double bar is in +sine phase and the light/dark is in –sine phase.

Stimulus presentation

The optimal orientation was determined by direct quantitative studies or sometimes, when it was so obvious, qualitatively by listening to the cells response to differently oriented bars or gratings. Stimuli were then presented at the optimal orientation to the dominant eye, the other eye being covered.

The presentation of grating stimuli was preceded by a uniform field for 1 s after which the grating contrast was ramped up from 0 to 0.3 over a 1 s period, held constant for 5 s and ramped down at the same rate. During the 3 s between trials, the spatial frequency or temporal frequency was changed, depending on the study being done. Spatial frequencies were tested in 0.5 octave steps. The stimulus order was newly randomized for each stimulus block and a neurone's respones to five to ten stimulus blocks were averaged to produce spatial and temporal frequency selectivity curves. Peak frequencies were determined using a cubic spline interpolation.

The stimulus block for bar studies consisted of four stimuli presented in the following order; light bar, dark bar, dark-light double bar and light-dark double bar. A neuron's responses to 50–100 stimulus blocks were averaged to produce response histograms to the four stimuli. At the viewing distance of 100 cm used in this study the height of the oscilloscope display subtended 5.7 deg and the width subtended 7.5 deg. The response histogram, which was measured as the bar stimuli traversed the width of the display, had 256 bins so that each bin corresponded to 0.029 deg.

Analysis of the data was done off line with the aid of the computer and programs developed in our laboratory. The spatial portion of the *mean* and its standard derivation for each average response histogram to the bar stimuli was calculated. The resolution of the position of the means depended upon the bin width (see above) which was narrow compared to the width of one full cycle of the subunits tested. The spatial offset of the means between pairs of histograms was determined from the differences between the respective means in degrees and then normalizing to a fraction of a cycle at the cell's preferred spatial frequency.

Results

Conventions and explanation of data display

In order to familiarize the reader with our conventions for data display, we review the operations involved in the successive stages of convolution of a stimulus and a subunit, response rectification, and (tentatively assumed) summation of rectified responses from adjacent subunits (Fig. 1A–E). The hypothetical line weighting function of subunits (Fig. 1) have been plotted as Gaussian-attenuated cosinusoid and sinusoids following the realization of Marcelja (1980) that the receptive field profiles of many simple cells closely approximated the elementary signals of Gabor (1946). The use of Gabor functions here provides computational convenience; their use need not imply that simple cells are the subunits that project onto complex cells nor that the subunits must be Gabor functions. The essential point here is the *even* or *odd* symmetry of the functions; several other functions would have served equally well. In these figures, as in the presentation

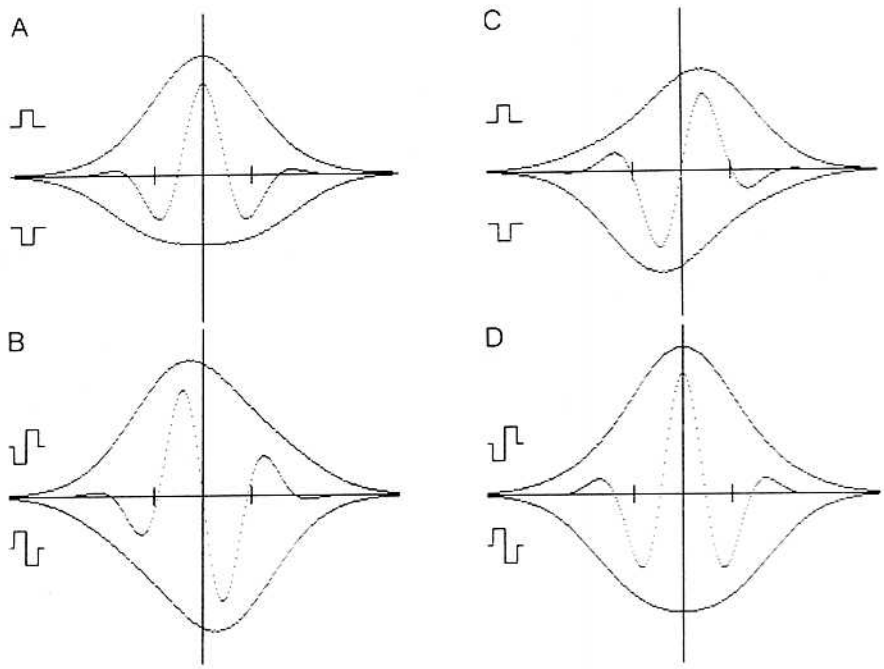

Fig. 2A–D. The responses of two model complex cells to single and double bar stimuli. The luminance profiles of each stimuli are shown to the left of each figure. The sum of all subunits, the complex cell response, is given by the outer lines in each figure. The responses to the lower stimulus in each figure are inverted. The model cells differ in the phase of their subunits; cosine phase (**A, B**), and sine phase (**C, D**). All other model parameters are the same for the two cells. Spatial frequency bandwidth = 1.5 octaves; subunits density = 16 subunits per cycle of the optimal spatial frequency. The distance between the tic marks on the x axes equals one cycle of the optimal spatial frequency of the subunit

of the actual data to follow, responses are shown as a combined histogram with those to the positive stimuli on top and those to the negative stimuli on the bottom and *inverted* (Fig. 1F).

The responses of two complex cells, one with exclusively ON-center even-symmetric subunits in cosine phase (Fig. 2A) and one with exclusively odd-symmetric subunits in sine phase (Fig. 2C) to each of the four stimuli themselves sequentially presented in +cos, –cos, +sin and –sin phase are shown in Fig. 2. The complex cell responses are shown as the envelopes in Fig. 2 and were generated by adding the responses of rectified subunits (shown inside the envelope) with adjacent axes of symmetry closely spaced at 1/16 cycle of the optimal spatial frequency with strengths on either side of the receptive field center decrementing according to a Gaussian with a standard deviation of 0.5 cycles. As discussed in Fig. 1, the curves below the x axis represent the inverted and rectified responses to the negative stimuli (dark bar and –sine phase double bars). However, because the figure convention inverts the response to a stimulus which is the inverse of the other stimulus, the curve inside the envelope can also be viewed as the response of a linear (unrectified) subunit to the upper left hand stimulus.

Data measures

Our examination of the complex cell subunits will concentrate on two measures: first, the relative response strengths to the different stimuli and second, the shapes of the combined histogram response to the two single bar and two double bar stimuli. To understand the relative response to the stimuli, we will first examine the responses of the individual subunits. Note that the response of a +cosine even-symmetric subunit to the single bar stimuli (the interior dotted line of Fig. 2A) has a greater positive than negative peak and total response. The converse would hold for a –cosine subunit. The differences in total response to the two stimuli, here in a ratio of 1.2 : 1, is characteristic of Gabor functions in this range of bandwidths. The ratio approaches 1.5 : 1 as bandwidth increases to two octaves. If the complex cell is made up of subunits of only type, then these same ratios should hold for the total response of the cell. One measure of interest will therefore be the relative response densities to single light and dark bars.

Second, note that the responses to the single bar stimuli retain the symmetry of the subunits the responses of even-symmetric subunits are even-symmetric themselves (Fig. 2A), those of odd-symmetric subunits are odd-symmetric (Fig. 2C). On the other hand, the double bar stimuli reverse the symmetry of the responses: the response of an even-symmetric subunit to the double bar stimulus is odd-symmetric (Fig. 2B), the response to the odd-symmetric subunit is even-symmetric (Fig. 2D).

The symmetry of the subunit responses has a direct influence on the shape of the combined response histograms. Whenever the subunits profiles

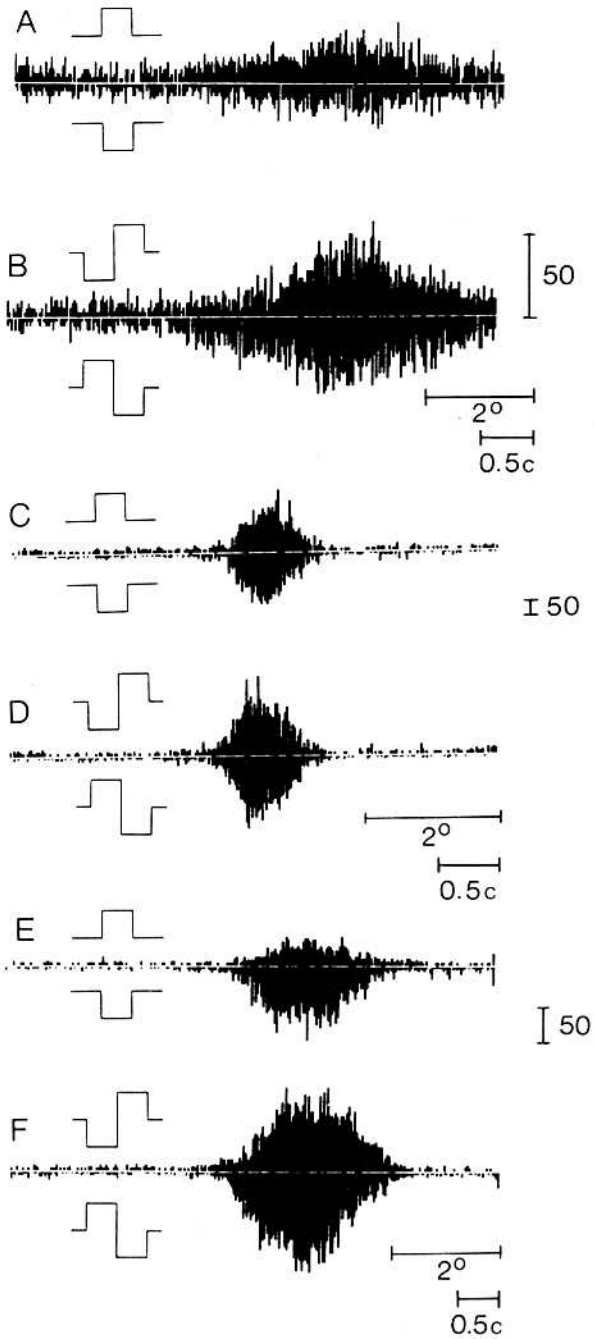

Fig. 3. A, B Greater response of a complex cell to a light bar (**A**, upper trace) than to a dark bar (**A**, lower trace). The responses to double bars in sine and –sine phase are shown as the upper and lower traces of **B. C, D** Approximately equal responses of a complex cell to light and dark bars (**C**) and equal but greater responses to the double bar stimuli (**D**). **E, F** This complex cell responds much more strongly to a dark bar (**E**, lower trace) than to a light bar. The total responses to the two double bars are about equal (**F**). The preferred spatial frequency of the cell in **A, B** is 1.4 c/d, in **C, D** is 2.0 c/d and in **E, F** is 0.7 c/d. One horizontal calibration bar indicates 0.5 cycles at the preferred spatial frequency here and in subsequent similar figures, and the other horizontal bar indicates 2° across the receptive field. The vertical bar is calibrated in impulses/second for the number shown

are odd-symmetric, there is a corresponding *offset* between the upper and lower response peaks of the combined response histogram. Whenever the subunits profiles are even-symmetric, there is no offset between the upper and lower response peaks. For a single subunit, measurements of the offsets between the peaks or *modes* would also provide reliable criteria for subunit type. However, for a neuron receiving input from multiple subunits, the offset between the modes is sensitive to the spacing interval and weighting function of the subunits as well as the subunit type. Hence, measurements of offsets based upon the mode cannot be reliably used to infer subunit type. On the other hand, as long as the type of subunit does not vary across the receptive field, the offsets between the *mean* are equal to the offsets of the subunits themselves, no matter what the subunit spacing or weighting.

The specific combination of subunit types contributing to a neuron's response can therefore be identified from the distinctive pattern of *offsets* observed in response to single and double bar stimuli. Our second measure of interest will therefore be the *offsets* evaluating the difference between the *means* of the upper and lower response distributions within the response pairs to single and double bar stimuli.

Response ratios of complex cells to single and double bars

We completed the entire experimental protocol on forty-four complex cells. The cell population includes recordings from four complex cells judged to be in V2 on the basis of a drop in preferred spatial frequencies to the 0.125–0.25 c/deg range as an electrode in one penetration advanced across the representation of the vertical meridian. All cells that we have considered "complex" satisfy the recent very strict criteria of Dean and Tolhurst (1983) with respect to both the "discreteness index" and the "modulation ratio". The complex cells also satisfied the original criteria of Hubel and Wiesel (1962) in that flashed stationary bars produced On-Off responses over most of the receptive field. In some penetrations, we recorded up to 6–8 complex cells before reaching the simple cell rich middle cortical layers. The vast majority of our complex cells were recorded from between 100–900 μ of the entry of the microelectrode into the cortex (see Methods). Although occasional simple cells were recorded at these depths, sequences of simple cells were only found at deeper levels. It is, therefore, probable but not certain that most of the complex cells we studied

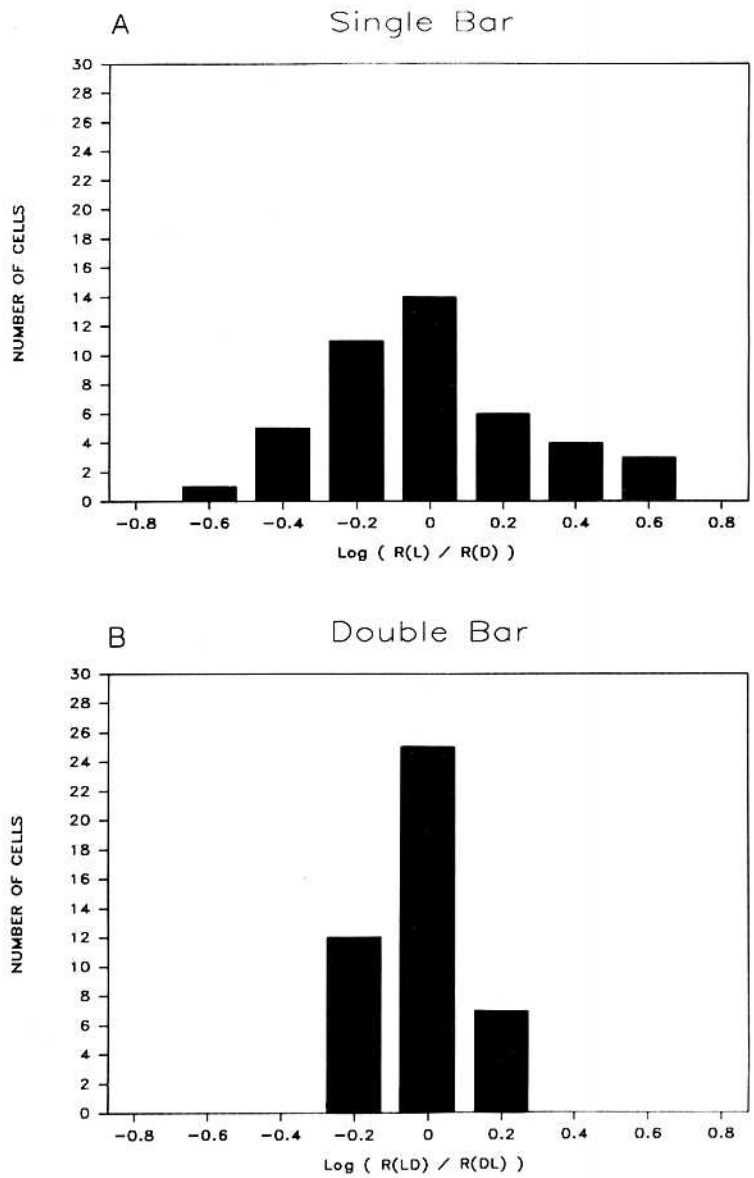

Fig. 4. A Number of cells as a function of the log of the ratio of the sum of the respective responses to light and dark bars. **B** Number of cells as a function of the log of the ratio of the sum to the respective responses to the double bars in sine and –sine phase.

were representative of the superficial cortical layers. Our simple cell population was studied for other purposes.

Widths of individual light and dark bars were set at one-quarter to one-half period of one cycle of the cell's preferred spatial frequency depending upon the minimum width necessary to obtain an adequate response density. The wider bars produced greater signal to noise ratios, but did not significantly affect response ratios to the two bars nor the shape of their respective average histograms.

Some complex cells respond much more strongly to drifting light bars than to dark bars of equal and opposite contrasts (Fig. 3A). Others respond about equally to light and dark bars (Fig. 3C). Still other complex cells respond much more strongly to dark bars than to light bars (Fig. 3E). Response ratios to the two polarities of stimuli often ranged from 1.5 : 1 to 2 : 1. At low contrasts close to threshold, the ratios could be exaggerated. In fact, as contrast was decreased, the cell of Fig. 3E, ceased to fire to a light bar, while still providing a strong response to a dark bar. Ratios stabilized at higher contrasts; consequently, all ratios reported (Fig. 4) are those obtained with our stimuli of highest contrast at 0.35.

Cells which responded to single bars but with substantially greater responses to either the light or dark bar were commonly found within single penetrations. Several cells with strong preferences for the light bars were often successively encountered as

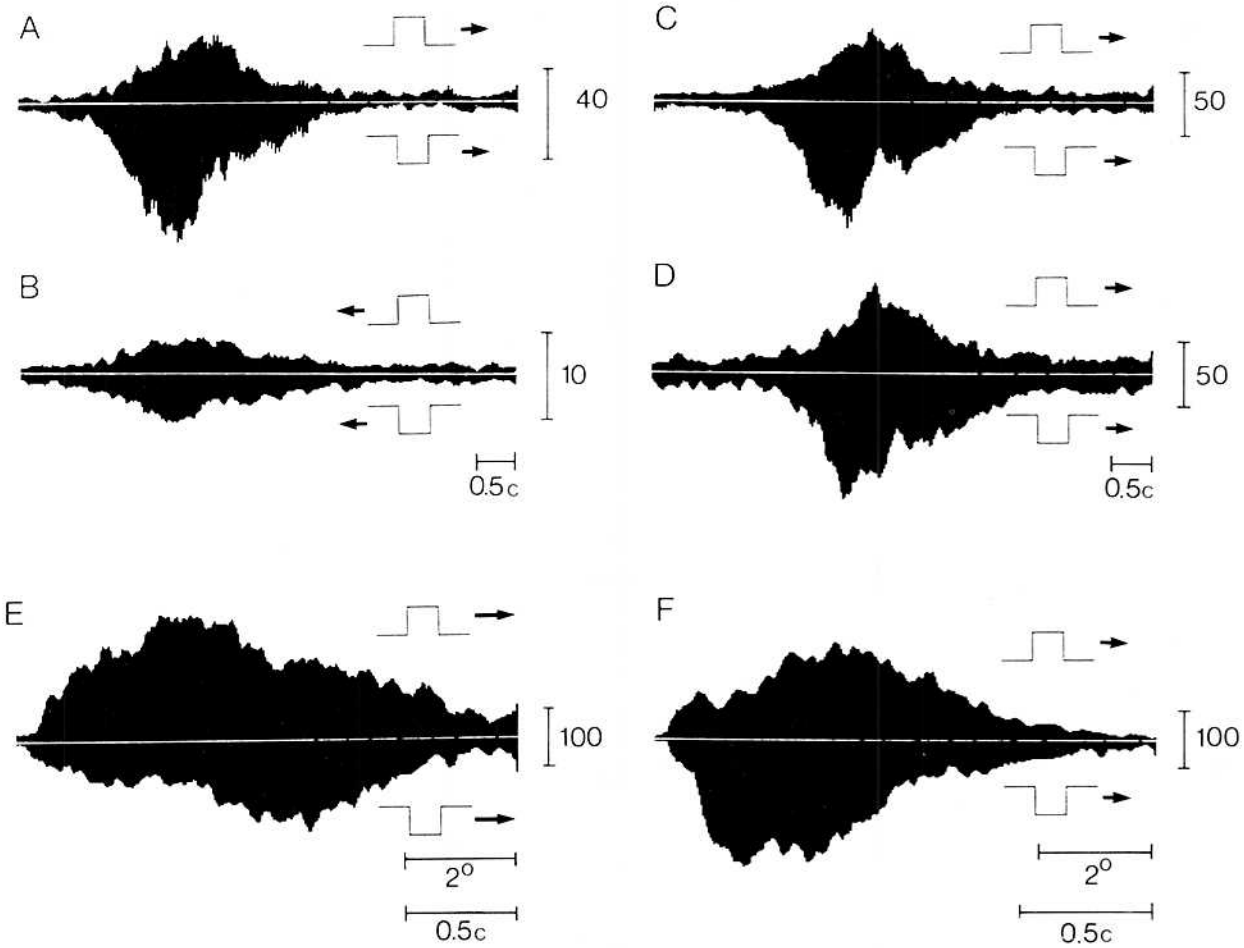

Fig. 5. A, B Responses of a complex cell to light and dark bars in one direction (**A**) and then in reverse direction (**B**). General shape of histograms, but not response density, is independent of direction. **C, D** Response of a complex cell to light and dark bars at 3.2 deg/s (**C**) and at twice that velocity (**D**). General shapes of the two sets of histograms are independent of velocity. **E,F** Records from adjacent cells in V2 which show opposite directions of offset in responses to light and dark bars. Preferred spatial frequency is 0.7 c/d in **A, B**, 0.7 c/d in **C, D**, 0.25 in **E** amd 0.21 in **F**. One set of horizontal bars indicates width of 0.5 cycle at the preferred spatial frequency. (The indicators of stimulus polarity have not been scaled for preferred spatial frequency)

were short strings of cells with preferences in the dark bars. We have not addressed the issue as to whether these segregations are columnar or laminar.

The distribution of the response ratios to single light and dark bars for all complex cells studied is shown in Fig. 4A. The data along the abscissa are plotted as the log of the ratio between the sum of the response to the light bar to that of the response to the dark bar. When these two response sums are about equal, the log of the ratio approaches zero, and the greatest number of cells cluster here. The number of cells which respond more strongly either to light or dark stimuli is about equal. The distribution is unimodal.

Asymmetries in the strength of the responses of complex cells to single light and dark bars have been implied since Hubel and Wiesel (1962) noted differential response strengths of ON and OFF responses to stationary flashed light bars. Movshon et al. (1978b) tested complex cells to stationary bright and dark bars at ten adjacent positions across the receptive field and found response differences to the two polarities of stimulation (their Fig. 6A, B) analogous to those we have found with drifting bars (Fig. 3A, E). Similar results have also been shown for complex cells in the striate cortex in the macaque monkey (Foster et al. 1985).

Responses of complex cells to narrow drifting odd-symmetric stimuli (double bars) are shown in (Fig. 3B, D, F). The distribution of the response ratios to the double bar stimuli (Fig. 4B) show less variance than the ratios for the light versus dark

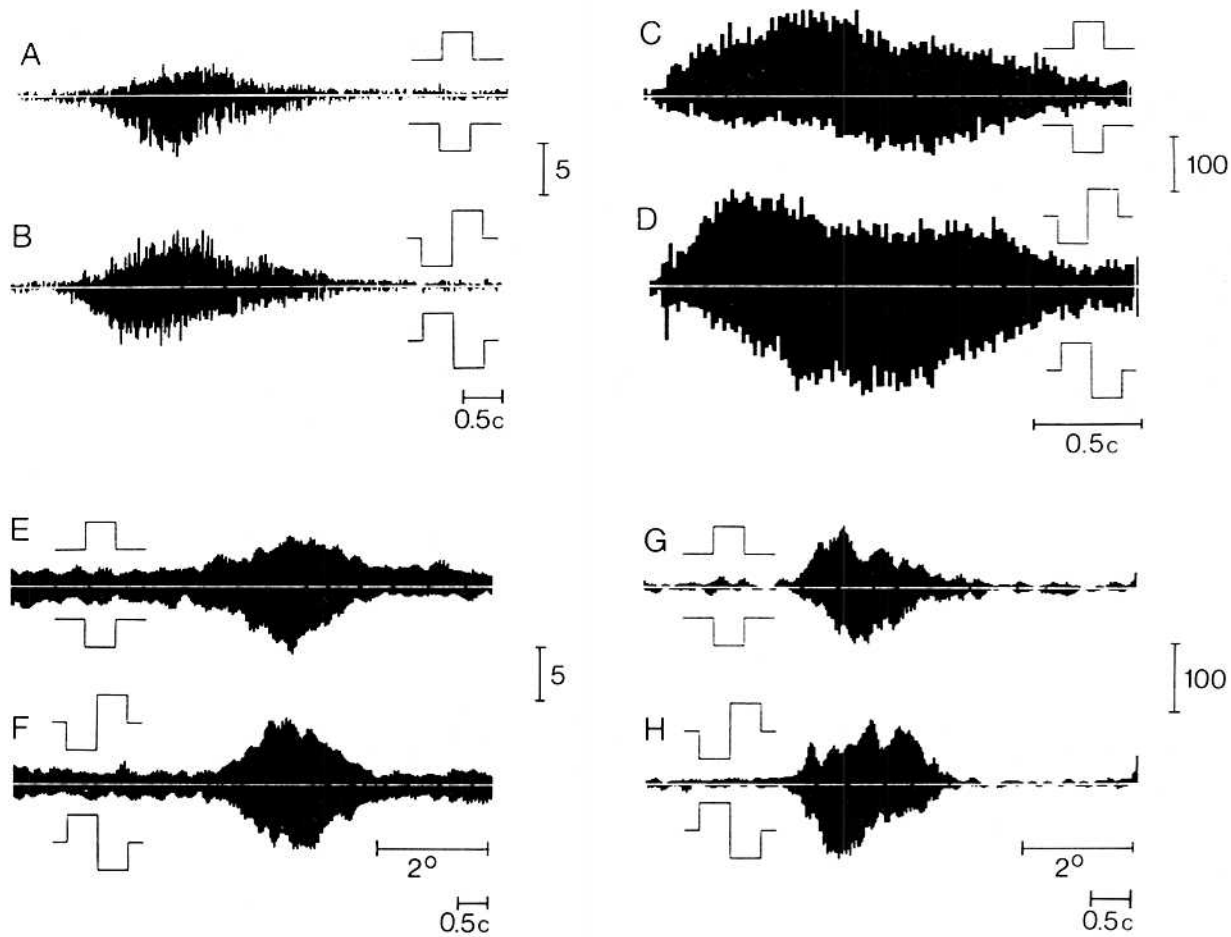

Fig. 6A–H. Responses of four complex cells (**A, B; C, D; E, F; G, H**) with different response patterns as described in text pairs of even-symmetric (**A, C, E, G**) and odd-symmetric stimuli (**B,D, F, H**). Display conventions as in Figs. 3, 5. Preferred spatial frequency is 0.7 c/d for cell in **A, B**, 0.25 c/d in **C, D**, 1.0 in **E, F** and 0.7 in **G, H**

single bars (Fig. 4A). This result and the greater total responses of cells to the double bars, are expected as the double bar contains more stimulus energy and it samples across both excitatory and inhibitory regions of each subunit thus averaging across any excitatory versus inhibitory differences. However, the position and strength of the peak response often depended upon the phase of the stimulus (i.e. +sine, dark/light or –sine, light/dark).

Spatial offsets between the response distributions of complex cells to single and double bars

A distinct type of response patterns to single light and dark bars was also seen. The modes of the individual response histograms were often spatially offset (Fig. 5A–F). The peak response to the light bar might be offset either to the right (Fig. 5A) or to the left (Fig. 5E) from the peak to the dark bar.

The direction of offset generally did not depend upon the direction of movement of the stimuli (compare Fig. 5A with 5B). The spatial offsets were not due to latency differences in the responses to light and dark bars because the same pattern of spatial offset appeared when the cells were tested at different velocities. For example, when a cell was tested with light and dark bars at velocities differing by a factor of 2, with both velocities being well within the preferred velocity range for the cell, the results show that the shapes of the average response histograms in the two cases are essentially similar (Fig. 5C, D). Thus, although directional and velocity factors may contribute to response strength, the asymmetries in the receptive field centers for the light and dark bars are indicative of a *spatial* substructure within the receptive field. In fact, offsets between responses to light and dark bars can be demonstrated with stationary stimulation in the cat (see Fig. 6D of Movshon et al. (1978b), Fig. 1F of

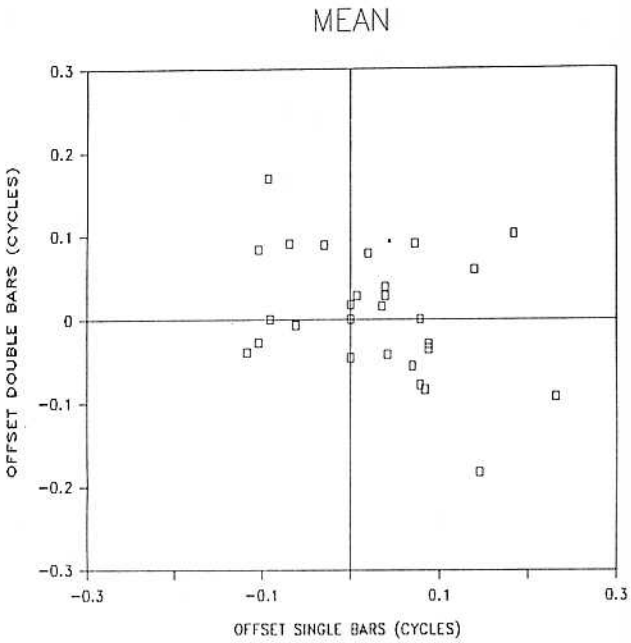

Fig. 7. The offsets between the means of the responses to single bars (abscissa) have been plotted against the offset to double bars (ordinate). The offsets have been normalized to cycles of the optimal spatial frequency of each cell

Dean and Tolhurst (1983) and Fig. 7B of Heggelund (1986)). Complex cells with distinct spatial offsets to drifting narrow light and dark bars are also found in V1 and V2 of the macaque monkey based upon our review of unpublished data from Foster et al. (1985). In both the cat and the macaque monkey, these cells can be either directionally or bidirectionally selective.

Successively encountered complex cells with the same orientation, spatial frequency and directional preference, might show equal and oppositely-directed spatial offsets (compare Fig. 5E with Fig. 5F). Sometimes, several successively encountered complex cells had a common direction of offset which then shifted for a subsequent cell.

Complex cells showing distinct spatial offsets in peak responses to the pair of single bars might show either "smooth" average response histograms (Fig. 6A) or show some evidence of discrete subunits contributions (Fig. 6G) as described for some complex cells by Pollen and Ronner (1975). The presence or absence of distinct subunit contributions appears to be a consequence of the regularity and density of subunit spacing and does not in other ways affect present results.

Some complex cells also showed spatial offsets to spatially-limited odd-symmetric (double bar) stimuli (Fig. 6B, D, F, H) as well as to the single bars (Fig. 6A, C, E, G). We found all combinations of directions of offsets to the single and double bars. For example, the response patterns to the pairs of single and double bars might be spatially offset in a common direction, with offsets to the right or to the left (Fig. 6, compare A, B, with C, D). Alternatively, the spatial offset to the single bars could be in the opposite direction (Fig. 6E, G) to that for the double bars (Fig. 6F, H).

The plot of the offsets of the spatial *means* of the responses to single bar stimuli versus those to double bar stimuli are shown respectively in Fig. 7. The calculation of the offset, normalized to cycles, depended upon an accurate determination of the cell's preferred spatial frequency. Only those cells were accepted for which the preferred spatial frequency could be estimated to at least one-quarter octave. Twenty-eight of the original forty-four cells satisfied these criteria. Offsets of the mean to single bar stimuli ranged from zero to 0.23 cycles and offsets to the double bars ranged from zero to 0.19 cycles.

In order to estimate the reliability of these points, several complex cells were studied more than once, using either identical stimulus conditions or stimuli which differed only in contrast. From six comparisons, the 95% confidence interval for these points was estimated as $\pm$ 0.098 cycles for single bar offsets and $\pm$0.133 cycles for double bar offsets. Eight of the twenty-eight points fall outside these confidence limits. The probability of finding eight or more cells outside these confidence limits by chance alone is extremely unlikely ($p < 0.0005$). This implies that the deviations from the origin of many of the points in Fig. 7 must be considered real. In addition to these cells that are outside the confidence limits, there are several cells clustered around the origin. Thus, any model of complex cell substructure must be able to account for this diversity of offsets.

Discussion

The diversity of response patterns to the test pairs of even- and odd-symmetric stimuli, which is often obvious on inspection and which has been quantified by the presence of data points in the combined offset plots along the axes, within all four quadrants and near the origin, implies considerable heterogeneity within the population of complex cells. The properties of complex cells as described here in the cat are likely to be of relevance to primate vision as well, since the same various patterns to single light and dark bars were seen upon re-examination of unpublished records from studies in the macaque monkey

by Foster et al. (1985). Moreover, similar patterns of complex cell response have been seen as far central as V4 of the macaque monkey (Desimone et al. 1985). We now inquire as to whether there are any models of complex cell substructure consistent with the present results.

Receptive field substructure

Specific models of subfield structure have already been proposed in the literature. Cavanagh (1984) and Spitzer and Hochstein (1985b) have suggested that all the subfields of a given cell may be of the same type. Specifically, Spitzer and Hochstein (1985b) have described complex cells made up of two or more positive even-symmetric subunits with various inter-subunit spacings. Cavanagh (1984) has proposed that for complex cells to preserve relative phase information, the subunits could be of any type, as long as all the subunits of a given complex cell were of the same type.

Spitzer and Hochstein (1985b) also proposed two other classes of complex cells where the subfields are made up of pairs of aligned subunits of opposite type. Their "B" cells, according to the classification of Henry (1977), are composed of a positive even-symmetric subunit aligned at its receptive field center with a negative even-symmetric subunit. The substructure of their "intermediate" class of complex cells is made up of two or more of these "B" cell pairs with an unspecified inter-pair spacing.

Pollen et al. (1985) have suggested that complex cell substructure could consist of the superposition of four types of subunits: positive and negative, even-symmetric subunits and left- and right-facing odd-symmetric subunits, all aligned along a common axis of symmetry.

Each of these proposals makes very specific predictions for the relations between offsets for single bars and those for double bars. In particular, any even-symmetric subunit will have the spatial mean of the response to the light bar aligned with that for the dark bar producing, therefore, no offset for single bars. On the other hand, the response of this subunit to a double-bar stimulus will be odd-symmetric as described above. There will be an offset between the mean of the response to the +sine, double bar and that to the –sine, double bar. This type of subunit, therefore, has a characteristic location along the y axis.

From these properties we can predict the expected single and double bar offsets for complex cells made up of subunits of a single odd- or even-symmetric type. These offsets should lie along the horizontal and vertical axes of the offset-offset plot. The amount of offset depends on the bandwidth of the cell (the narrower the bandwidth, the greater the number of extra lobes and the less the offset) but the direction does not.

When subunits are combined in pairs of opposite types, exactly aligned as suggested by Spitzer and Hochstein (1985b), the spatial means of the response histograms are necessarily aligned for both single and double bar stimuli. Therefore, these cells are expected to fall at the origin of the offset-offset plot. Similarly, complex cells made up of two pairs of subunits of opposite type, one pair even-symmetric (one +cosine and one –cosine) and the other odd-symmetric (one +sine and one –sine), will also produce no offsets for either single or double bar stimuli. They should also fall at the center of the offset-offset plot.

It is clear in Fig. 7 that the points do not cluster around specific values. It may be that those few cells whose points fall along the axes correspond to a model consisting of a single type of even- or odd-symmetric subunit across the receptive field (Cavanagh 1984). The few points close to the origin may correspond to models proposing paired subunits of opposite type as outlined above by Spitzer and Hochstein (1985b) and Pollen et al. (1985). Even if this is true, there are evidently many other data points that do not fit the two types of models just described.

Alternative substructures

There are at least two potential complex cell substructures that could produce the scatter of the points away from the origin and axes seen in Fig. 7. First, the subunits of the complex cells may have sensitivity profiles of mixed symmetry, that is, neither of even nor odd symmetry but of some intermediate "phase" (where "phase" refers to the phase of the sinusoidal variation in sensitivity relative to the center of the Gaussian envelope of the subunit's sensitivity profile). In this case, the subunits could still be all of one type of "phase" (Cavanagh 1984). The offset-offset points for these cells would then fall along a direction from the origin determined by the phase of the subunit's sensitivity profile, and at a distance determined by the bandwidth. If this were the case, the data would imply that there is a uniform distribution of phases of the underlying sensitivity profiles as well as cells with points near the origin that must be made up of pairs of subunits of opposite type. A similar result seems to hold at the simple cell stage in that McLean-Palmer et al. (1985) and Heggelund (1986)

have shown that the distribution of phases of the receptive field profiles of simple cells is approximately uniform.

Second, the substructure for cells with points along the diagonals might also consist of aligned pairs of odd- and even-symmetric subunits. For example, the combination of a sine- and a cosine-phase subunit will produce responses whose points fall along the diagonals of the offset-offset plot. Combinations of the sine and cosine subunits with different weights could produce offset-offset points at any particular direction from the origin depending on the weights. These same arguments are not limited to only odd- and even-symmetric subunits but can be extended to aligned pairs of subunits whose profile phases differ by 90°.

It is not difficult to generate many other variations of complex cell substructure but, with the exception of those already mentioned, other possibilities either produce offset-offset points that vary only along two axes and do not fill all possible directions or they involve subfields that vary in sensitivity profile across the complex cell receptive field. The first of these can be ruled out by our data, but the second cannot.

Acknowledgements. We sincerely thank Miss Cindy Wilson for her technical assistance and Dr. Robert A. Lew for his expert help with statistical problems. We also thank Professor Richard Kronauer and Terry Sanger for their extremely helpful criticism and comments. This work was supported by USPHS grant EY05156 from the National Eye Institute to D.A.P. and Natural Sciences and Engineering Research Council of Canada grant A8606 to P. C.

References

Andrews BW, Pollen DA (1979) Relationship between spatial frequency selectivity and receptive field profile of simple cells. J Physiol 287: 163–176

Cavanagh P (1984) Image transforms in the visual system. In: Dodwell PC, Caelli TM (eds) Figural synthesis. Lawrence Erlbaum Associates, Hillsdale New Jersey

Desimone R, Schein SJ, Moran J, Ungerleider LG (1985) Contour, color and shape analysis beyond the striate cortex. Vision Res 25: 441–452

Dean AF, Tolhurst PJ (1983) On the distictntiveness of simple and complex cells in the visual cortex of the cat. J Physiol 344: 305–325

DeValois KK, Tootell RBH (1983) Spatial-frequency-specific inhibition in cat striate cortex cells. J Physiol 336: 359–376

Foster KH, Gaska JP, Nagler M, Pollen DA (1985) Spatial and temporal frequency selectivity of neurons in visual cortical areas V1 and V2 of the macaque monkey. J Physiol 365: 331–363

Gabor D (1946) Theory of communication. J Inst Electr Eng 93: 429–459

Heggelund P (1986) Quantitative studies of the discharge fields of single cells in cat striate cortex. J Physiol 373: 277–292

Henry GH (1977) Receptive field classes of cells in the striate cortex of the cat. Brain Res 133: 1–28

Hubel DH, Wiesel TN (1962) Receptive fields, binocular interaction and functional architecture in the cats visual cortex. J Physiol 160: 106–154

Maffei L, Morrone C, Pirchio M, Sandini G (1979) Responses of visual cortical cells to periodic and non-periodic stimuli. J Physiol 296: 27–47

Marcelja S (1980) Mathematical description of the responses of simple cortical cells. J Opt Soc Am 70: 1297–1300

McLean-Palmer J, Jones J, Palmer L (1985) New degrees of freedom in the structure of simple receptive fields. Invest Ophthalmol Vis Sci Suppl 26: 265

Movshon JA , Thompson LD, Tolhurst DJ (1978a) Spatial summation in the receptive fields of simple cells in the cats striate cortex. J Physiol 283: 53–77

Movshon JA, Thompson ID, Tolhurst DJ (1978b) Receptive field organization of complex cells in the cats striate cortex. J Physiol 283: 79–99

Pollen DA, Foster KH, Gaska JP (1985) Phase-dependent responses of visual cortical neurons. In: Rose D, Dobson V (eds) Models of the visual cortex. John Wiley, Chichester, pp 282–291

Pollen DA, Ronner SF (1975) Periodic excitability changes across the receptive fields of complex cells in the striate and parastriate cortex of the cat. J Physiol 25: 667–697

Spitzer H, Hochstein (1985a) A complex cell receptive field model. J Physiol 53: 1266–1285

Spitzer H, Hochstein (1985b) Simple and complex-cell response dependences on stimulation parameters. J Neurophysiol 53: 1244–1265

Received June 9, 1986 / Accepted April 22, 1987